MODELING MODERN AND LATE PLEISTOCENE GLACIO-CLIMATOLOGICAL CONDITIONS IN THE NORTH CHILEAN ANDES (29–30° S)

CHRISTOPH KULL [1,2], MARTIN GROSJEAN [3] and HEINZ VEIT [1]

[1] *Geographical Institute, University of Berne, Physical Geography, Hallerstrasse 12, 3012 Berne, Switzerland*
E-mail: kull@giub.unibe.ch
[2] *PAGES IPO, Bärenplatz 2, 3011 Berne, Switzerland*
[3] *NCCR Climate, Erlachstrasse, 3012 Berne, Switzerland*

Abstract. An empirical-statistical climate-glacier model is used to reconstruct Late Pleistocene climate conditions in the south-central Andes of northern Chile (29–30° S). The model was tested using modern climate data and the results compare favorably with key glaciological features presently observed in this area. Using several glaciers at 29° S as case studies, the results suggest an increase in annual precipitation ($\Delta P = 580 \pm 150$ mm, today 400 mm), and a reduction in annual mean temperature ($\Delta T = -5.7 \pm 0.7$ °C). These data suggest full glacial LGM (Last Glacial Maximum) conditions for the maximum glacier advances at 29° S, a scenario that is asynchronous with the timing of maximum advances north of the Arid Diagonal (18–24° S) where late-glacial climate was moderately cold but very humid.The reconstructed case study glaciers at 29° S do not allow conclusions to be drawn about the seasonality of precipitation. However, comparison with regional paleodata suggests intensified westerly winter precipitation and a stable position for the northern boundary of the westerlies at ~27° S. However, the meridional precipitation gradients were much steeper than today while the core area of the Arid Diagonal remained fixed between 25–27° S.

1. Introduction

The arid Central Andes have become a key site for the study of abrupt and high-amplitude climatic changes during late Pleistocene and Holocene times. This arid transition zone (Arid Diagonal, 25–27° S) is located between the tropical and extra-tropical circulation systems, and this makes it an ideal system to study changes in large-scale atmospheric circulation patterns (Messerli et al., 1996). Today, this area is extremely arid. Due to the lack of moisture, perennial snowfields and glaciers are absent between 20° S and 27° S even in the continuous permafrost belt above 5600 m.

Whereas the last maximum glacial advances north of the Arid Diagonal (18–25° S) are confirmed to be late-glacial in age, when conditions were moderately cold and very humid (Hastenrath and Kutzbach, 1985; Clayton and Clapperton, 1997; Kull and Grosjean, 2000), the timing and the paleoclimatic conditions (extratropical winter or tropical summer precipitation) during the maximum glacier expansion immediately south of the Arid Diagonal (29–30° S) are not known yet.

Climatic Change **52:** 359–381, 2002.

This is, however, the key to better understand the different climatic regimes north and south of the Arid Diagonal, and provides insight into the dynamics of the tropical and extratropical circulation belts.

In this study, a glacier-climate model (Kull, 1999; Kull and Grosjean, 2000) is used to reconstruct climate conditions for the maximum late Pleistocene glacier extensions immediately south of the Arid Diagonal at two adjacent test sites in the Encierro valley (29°11′ S, 69°57′ W, Figure 1). In combination with the available paleoclimate history from other archives (lake and marine sediments, ice cores, pollen profiles and paleosols; Thompson et al., 1995, 1998; Veit, 1995, 1996; Jenny and Kammer, 1996; Clayton and Clapperton, 1997; Geyh et al., 1999; Bradbury et al., 2001; Grosjean at al., 2001), we present an overview for the lively Late Pleistocene history of the tropical and extratropical circulation belts in the Central Andes of northern Chile (18–30° S).

2. Research Area, Modern Climate and Glaciological Conditions

The research area is located in the high Central Andes of Northern Chile near the boundary with Argentina between 29 and 30° S (Figure 1). South of the Arid Diagonal, precipitation on the western side of the Andes at 4000 m increases from 100 mm a^{-1} at 26° S to 400 mm a^{-1} at 30° S (Minetti et al., 1986; Ammann, 1996; Vuille and Ammann, 1997), and winter precipitation with Pacific moisture related to cyclone activity becomes dominant. The summer months are dry, although sporadically interrupted by convective showers from the continental eastern side of the Andes (Table I). The southward increase in precipitation is also manifested in the presence of isolated glaciers south of 27° S, where ELAs (Equilibrium Line Altitude) decrease from 5900 m at 27° S to 5300 m at 30° S and to 4500 m at 32° S (Hastenrath, 1971). Co. Tapado (30° S, 5550 m), glaciated as low as 4600 m, exists due to this precipitation increase. However, higher peaks adjacent to Co. Tapado, such as Co. Olivares (30°17′ S 69°54′ W, 6252 m), are currently free of glaciers, suggesting that some of the existing glaciers are atypical features in this area and that local climatic conditions (e.g., excess precipitation) play an important role.

Global radiation, wind speed, humidity and temperature were measured using an automated weather station near the Cerro Tapado base camp (30°08′ S, 69°55′ W, 4215 m, Figures 2 and 3) during 1998/99 and on the summit plateau of the glacier at 5500 m during an ice-coring campaign between February 11–16, 1999 (Figure 2). We used the period where data from both stations overlap to establish correlation models and lapse rates. These allowed us to calculate an annual cycle for the summit plateau based on the data from the lower station. The agreement between measured and calculated data on the summit is $r^2 = 0.9$.

In the currently ice-free Encierro valley (29°11′ S, 69°57′ W), late Pleistocene glaciation was widespread and included surprisingly long valley glaciers, some up to 14 km in length. The topographical setting of the two selected glacier beds (Las

Table I
Modern climatic conditions in the research area

CLIMATE	Precip. (P) [d,f]	Temp. (T) [a,f]	Radiation (G) [a,f]	Wind (W) [a,b,c]	Rel. hum. (RH) [a,b,c]	Cloudiness (C) [e]
Annual mean	400	–0.4	5.62	4.36	28	15
Annual amplitude	(summer 100 mm)	6	2.1	2	3	5
Daily amplitude (Da)		8				
Lapse rate	12	–0.68 (summer)	0.04	0.08	0.09	0.84
(/100 m)		–0.71 (winter)				

[a] Tapado 4215 m (30°08′ S/69°55′ W; 1998–1999).
[b] El Laco 4400 m (23°50′ S/67°29′ W; 1990–1994).
[c] El Laco 5000 m (23°50′ S/67°29′ W; 1990–1994).
[d] Minetti et al. (1986).
[e] Ammann (1996).
[f] Vuille (1996).

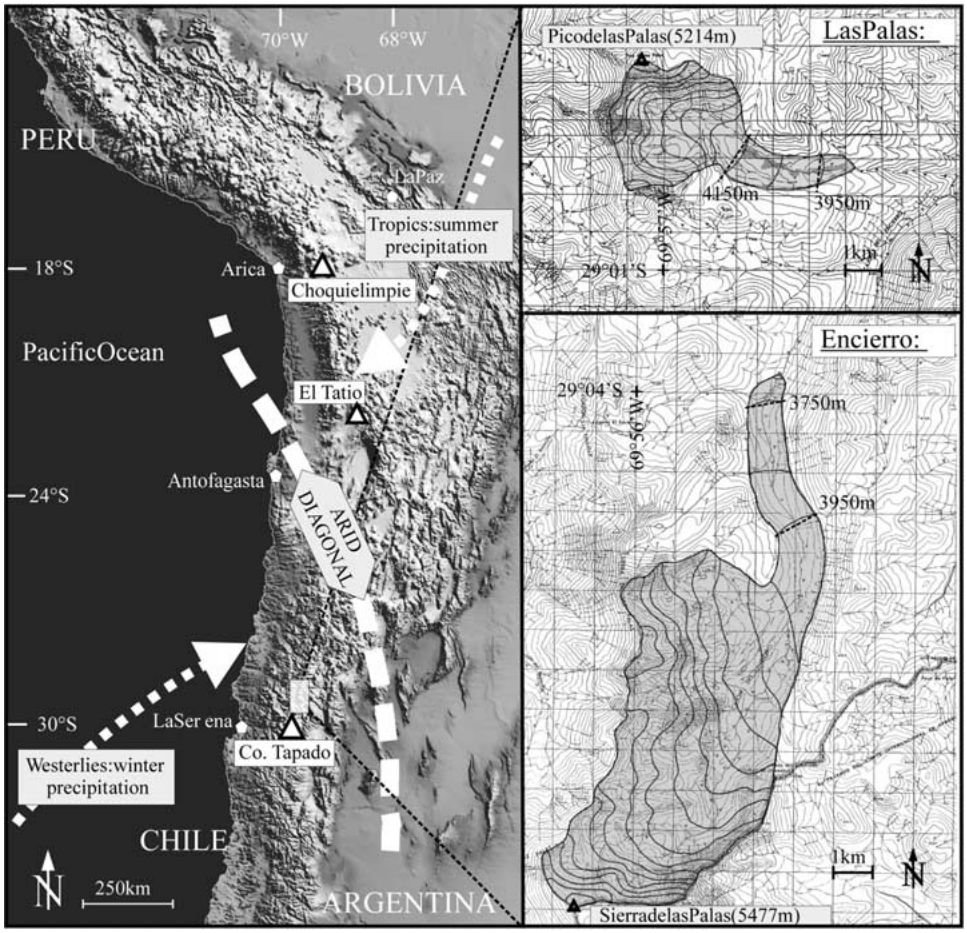

Figure 1. Map showing the location of the two case-study glaciers Encierro and Las Palas in the Encierro valley (29° S) in the Andes of northern Chile south of the Arid Diagonal. The lines represent reconstructed ice isohypses (100 m interval), the dotted lines show the cross-sections used in the model.

Palas and Encierro, Figure 1) is ideal for modeling because the slopes of the glacier beds are uniform and gentle (between 4° and 6°), the topography is relatively simple and the watershed boundaries and glacial deposits are clearly identifiable.

For the modeling process, trapezoidal cross-sections were reconstructed at two different altitudes (Encierro at 3750 m and 3950 m; Las Palas at 3950 m and 4150 m, Figure 1). The aspect of the former glaciers is N-S (Encierro) and W-E (Las Palas). Detailed mapping of the glacier deposits (Jenny and Kammer, 1996) and the simple geometry of the glacier beds fulfill the prerequisites for the glacier-climate model.

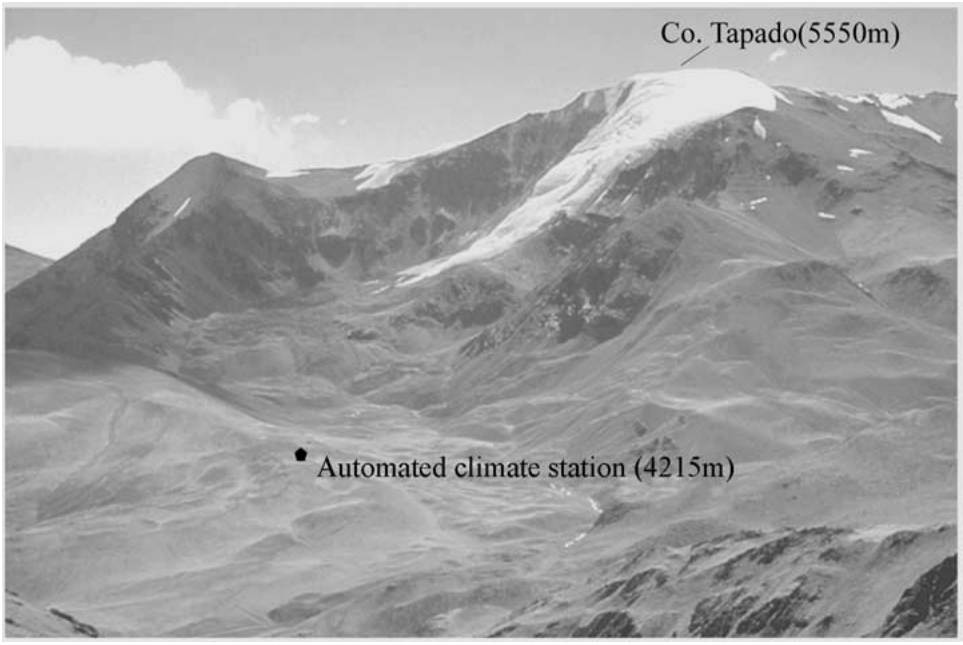

Figure 2. Glacier on Cerro Tapado (30°08′ S, 69°55′ W, 5550 m) in the North Chilean Andes near the border to Argentina (Photo: 3.3.1990). A 39 m long ice core was taken on the summit plateau in February 1999.

3. The Model

Model input includes: (i) a detailed geometry of the modern glacier or the late Pleistocene maximum glaciation as mapped in the field (Figure 1), (ii) modern diurnal and annual cycles, amplitudes and lapse rates of the climate (Tables I and IIa), (iii) empirical-statistical sublimation-, melt- and accumulation models developed for this area (Table IIb, Kull, 1999), and (iv) dynamic ice flow calculations through two known cross-sections under steady-state conditions (Table IIc, Kull, 1999). For a detailed discussion of the model see Kull (1999) and Kull and Grosjean (2000).

The actualistic principle is used as the basis and prerequisite for modeling mass balance changes as a function of the climate. The mass balance terms 'melt' 'sublimation' and 'accumulation' are calculated for individual altitudinal segments of the glacier and checked with field data (Tables IIb and III, Figures 4–6). The mass flow (Oerlemans, 1997) is calculated for given cross-sections (Figure 1) within the reconstructed glacier bed (Table IIc). In order to fulfill steady-state conditions for the modeled glacier, the differences between the mass balance below each of the considered two cross-sections and the mass influx into the considered cross-sections (DMM) of each glacier must be zero. Finally, the climate scenario is tuned (iteration) in such a way that the model glacier is in steady-state conditions (total

Table IIa

(a) Parameterization for the daily, annual cycles, amplitudes of the climate and correction factors for temperature and global radiation (Kull and Grosjean, 2000)

MODEL EQUATIONS:			
Climate:			
Temperature [a,d,f]	$T_{t,h}$ [°C]:	$T_{t,h} = Ym + Ya(\cos d) + (Da + C^*)\cos t + grad_h + P^*$	
Cloudiness [c]	$Cs_{t,h}$ [%]: (summer)	$Cs_{t,h} = Ym + Ya(\cos d_s) + Da(\cos t_s) + grad_h$;	$0 < Cs < 100$
	$Cw_{t,h}$ [%]: (winter)	$Cw_{t,h} = Wm + Wa(\sin d_w) + grad_h$;	$0 < Cw < 100$
Precipitation [c,d,f]	$Ps_{t,h}$ [mm]: (summer)	$Ps_{t,h} = 0.161Cs_{t,h}^2 + 0.81Cs_{t,h} + grad_h$	
	$Pw_{t,h}$ [mm]: (winter)	$Pw_{t,h} = Wm(Cw_{t,h}\,Wm^{-1}) + grad_h$	
Rel. humidity [a,b,f]	$RH_{t,h}$ [%]:	$RH_{t,h} = Cs_{t,h} + Cw_{t,h} + grad_h$	
Wind speed [b]	$W_{d,h}$ [m s^{-1}]:	$W_{d,h} = Ym + Ya(\sin d) + grad_h$	
Global radiation [b,d]	$G_{d,h}$ [W m^{-2}]:	$G_{d,h} = Ym + Ya(\cos d) + C^* + T^* + grad_h$	
Deg.-day-fac. [d,e]	$DDF_{d,h}$ [mm °C^{-1} d^{-1}]:	$DDF_{d,h} = Ym + Ya(\cos d)\cos h + grad_h \sin h$	
Corrections:			
Temperature:	P^* [a]: Correction term due to precipitation, $\Delta T = -4$ °C if $P > 0$.		
	C^* [a]: Correction term due to cloudiness, $\Delta Da = -0.03 \cdot C$ [%].		
Global radiation energy	C^* [b]: Correction term due to cloudiness, $\Delta G = 0.25 \cdot C$ [%].		
	T^*: Correction term due to radiation shielding (topography).		
Da : daily amplitude	Ya : annual amplitude	Ym : annual mean value	
$grad_h$: lapse rate (h/100 m)	C^*: cloudiness corr.	P^* : precipitation corr.	
T^* : topographic corr.	d_s : days in summer (Oct–Mar) [$f(t)$]	d_w : days in winter (Apr–Sep) [$f(t)$]	
Wm : winter mean value	t : hours	t_s : hours in summer	
Wa : winter amplitude	h : altitude	d : days [$f(t)$]	

[a] El Tatio 4320 m (22°21′ S/68°02′ W; 1977–1994).
[b] El Laco 5000 m (23°50′ S/67°29′ W; 1990–1994).
[c] Ammann (1996).
[d] Vuille (1996).
[e] Sicart and others (1998), Wagnon and others (1999).
[f] Chungara Ayata 4570 m (18°14′ S/69°20′ W; 1984–1994).

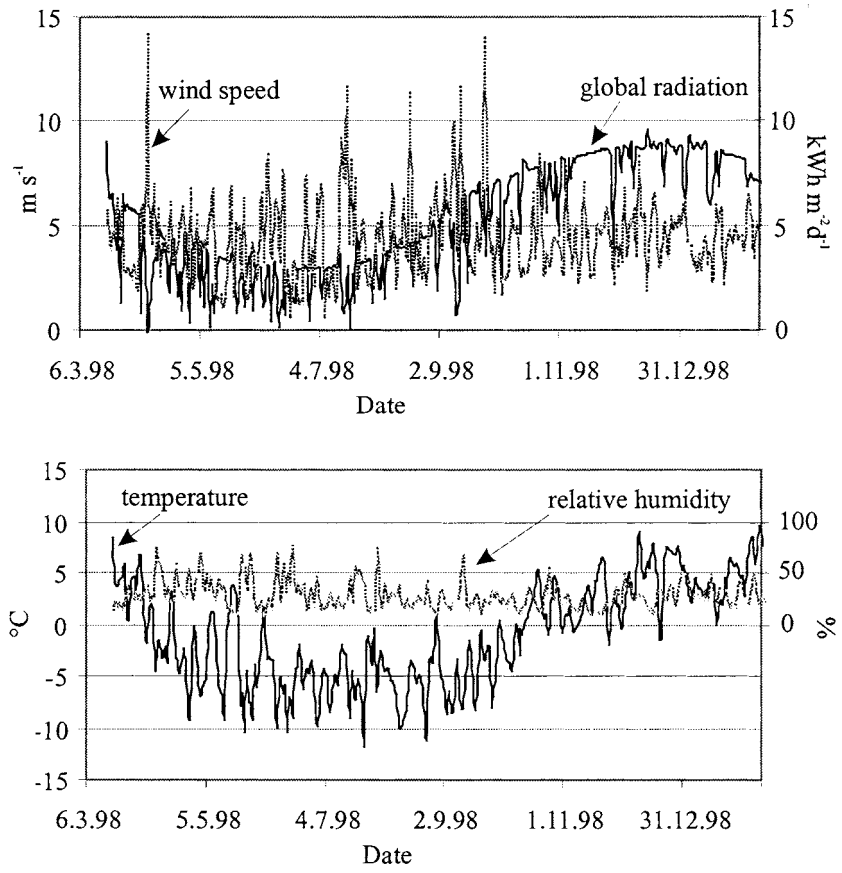

Figure 3. Measured climate conditions (mean daily values) for an annual cycle 1998–1999 at the base station of Cerro Tapado at 4215 m a s l.

mass balance is zero, DMM is zero) and in equilibrium with the prevailing climate or paleoclimate, and matches the corresponding glacier geometry.

The sensitivity of the results is tested as described in Kull and Grosjean (2000) and allows for an error of $\pm 20\%$ for the ice flow parameters (Table IIc) and $\pm 10\%$ for the geometrical reconstruction of the glacier bed (ice height, bed width, slope angle of the valley; Figure 1).

As a further development of this model, the modeled temperature changes ΔT are divided into local effects due to local cloudiness and local precipitation (latent heat), and regional effects (e.g., temperature of the advected air masses). The local effects are calculated using the correction terms for cloudiness and precipitation (Table IIa, Kull, 1999) as computed from station data.

$$\Delta T = \Delta T_{\text{local}} + \Delta T_{\text{regional}} \tag{1}$$

Table IIb

(b) Empirical-statistical models developed in the research area for the mass balance modeling (Kull and Grosjean, 2000)

MASS BALANCE:				
Sublimation[a]	$subl_{d,h} = --1.33 + 0.12(W_{d,h}) + 0.24(Dd_{d,h}) + 0.27(G_{d,h})$			[mm d^{-1}]
	with:	$W_{d,h}$:	max. hourly wind velocity (daily average)	[m s^{-1}]
		$Dd_{d,h}$:	mean daily vapour pessure deficit	[hPa d^{-1}]
		$G_{d,h}$:	daily global radiation energy	[W m^{-2}]
Melt[a]	$melt_{d,h} = 0.97 + DDF_{d,h}(Tg_{t,h})$; for $Tg > 0$			[mm d^{-1}]
	with:	$Tg_{t,h}$:	hourly means of the positive temperatures per day	[°C]
		$DDF_{d,h}$:	degree-day-factor, f (albedo, snow density, climate)	[mm °C^{-1} d^{-1}]
Accumulation[b]	$acc_{d,h} = \frac{1}{24}\sum_{t=24d}^{24+24d} \begin{cases} P_{t,h}; & \text{if } T_{t,h} < 2 \\ \left(\frac{4 - T_{t,h}}{2}\right) P_{t,h}; & \text{if } 2 \leq_{t,h} \leq 4 \\ 0 & \text{otherwise} \end{cases}$			[mm d^{-1}]
	with:	$P_{t,h}$:	hourly precipitation	[mm]
		$T_{t,h}$:	hourly mean temperature	[°C]
Specific annual mass balance	$b_h = \sum_d -(subl_{d,h} + melt_{d,h}) + acc_{d,h}$			[mm a^{-1}]

[a] Vuille (1996).
[b] Kull (1999).

with: ΔT = modeled total temperature (°C); ΔT_{local} = local temperature change due to variations in cloudiness and latent heat if moisture is available (°C); $\Delta T_{\text{regional}}$ = regional temperature change (°C).

4. Results and Discussion

We first tested the model with the modern glacier on Cerro Tapado (Figure 2, 30°08′ S, 69°55′ W, 5550 m). Then the model was used to reconstruct the climatic conditions required to produce the two late Pleistocene case study glaciers in the adjacent Encierro valley to the north (Figure 1). The results allow us to draw some conclusions about the regional atmospheric circulation pattern during the late Pleistocene period.

4.1. THE RECENT GLACIATION ON CERRO TAPADO

The glacier on the SE slope of Cerro Tapado ranges from the summit plateau at 5550 m to a lowest point at 4600 m, and covers approximately 150 ha. The maximum thickness is 40 m, and the modern ELA is found at 5300 m. Using

Table IIc

(c) Equations for the ice flow and mass flux calculation for the considered cross-sections in the two case-study glaciers (Kull and Grosjean, 2000)

ICE FLOW:			
Flow velocity[a]	$U = U_d + U_s$		[m s^{-1}]
	$= f_d H \tau^3 + \frac{f_s \tau^3}{H}$		
	with:	$\tau = -FpgH\beta$ = mean basal shear stress in cross-section[b]	[Pa]
		$F = \frac{Q}{HB}$ = form factor[c]	[%]
		Q = cross section area	[m^2]
		B = hydraulic radius	[m]
		U = mean ice velocity in the cross-section	[m s^{-1}]
		U_d = deformation velocity	[m s^{-1}]
		U_s = sliding velocity	[m s^{-1}]
		f_d = flow parameter (internal deformation)	[$1.9 \cdot 10^{-24}$ Pa^{-3} s^{-1}]
		f_s = flow parameter (basal sliding)	[$5.7 \cdot 10^{-20}$ Pa^{-3} m^2 s^{-1}]
		H = ice thickness	[m]
		p = ice density	[900 kg m^{-3}]
		g = acceleration due to gravity	[m s^{-2}]
		β = bed slope	[%]
Cross section mass influx	$M = UQp$		[kg s^{-1}]

[a] Oerlemans (1997).
[b] Paterson (1994).
[c] Budd (1969).

our data from the weather station at 4215 m and respective lapse rates, the model calculated mean sublimation rates of 1.89 mm d^{-1} for the period between February 11–16, 1999 (Figure 4a, Table III) at 5500 m. The annual cycle of daily sublimation between 1998/99 (Figure 4b) shows, that sublimation is particularly high during the dry cloud-free summer months with intense radiation. The model calculated a cumulative sublimation between September 1998 (end of the winter season) and February 1999 of 320 mm water equivalent.

Using modern climate data for one annual cycle (Table I, mean regional annual precipitation rates of 400 mm at 4000 m, 580 mm at 5500 m) the model results suggest that, due to the high ablation rates of 650 mm a^{-1} at 5500 m (mainly sublimation), the mass balance is negative over all the altitudinal belts up to 6000 m. Thus, an ELA generally does not exist within this range because the climate is still too dry for glacier survival (Figure 5a). Indeed, the mountains adjacent to Co. Tapado are as high as 6000 m and currently free of glaciers, confirming the model results. Surprisingly, the glacier on Co. Tapado exists under current climatic conditions. The model suggests (Figure 5b) that this particular glacier requires additional local accumulation, on the order of 170 mm a^{-1} higher than the regional values (i.e., total accumulation of 750 mm a^{-1} at 5500 m instead of regional 580 mm a^{-1})

Table III

Summary of glaciological data and mass balance terms for the Tapado glacier on the summit plateau (5550 m), collated from field data, ice core stratigraphy, enrichment factors of chemical species and radio isotope data from the ice core.

	ELA	Sublimation (15.9.1998–16.2.1999)	Mean daily sublimation (11.2.–16.2.99)	Melt	Net accumulation	Mean annual temperature (5250 m)
	m a s l.	mm weq	mm d^{-1} weq	mm a^{-1} weq	mm a^{-1} weg	°C
Field data	~5300		1.89	Little frozen lakes		
Ice core [a]				Ice lenses	290	
Chem. analysis [a]		310	1.85			
Temp. logger [a]				Pos. temperatures in summer		–9.1
Modeled values	5280	320	1.89	60	260	–9.7

[a] Ginot and others, submitted.

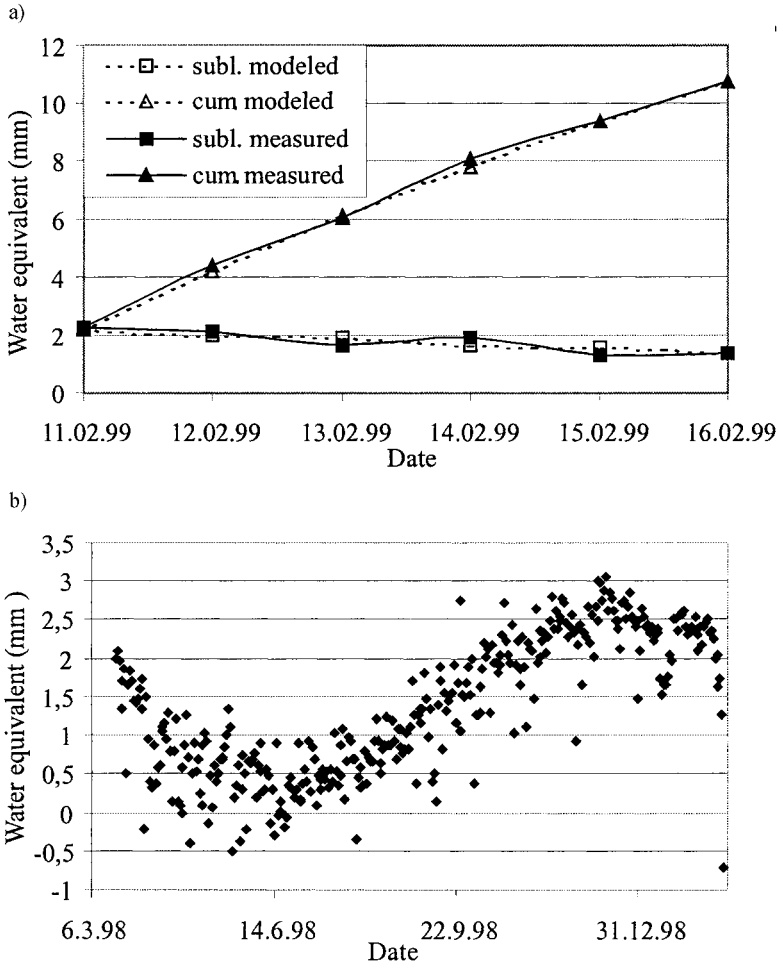

Figure 4. (a) Comparison between the measured and modeled daily sublimation values (subl. measured, subl. modeled) on Cerro Tapado during the ice drilling campaign in February 1999. The cumulative values (cum. modeled, cum. measured) suggest that there is no systematic error between measured and modeled sublimation. (b) Showing the modeled daily sublimation values for the summit plateau of Cerro Tapado (5550 m) during the annual cycle 1998/99. A total amount of 490 mm for this year indicates that sublimation is the most important ablation term.

to match the observed ELA at 5300 m. Thus, given the modeled annual sublimation of 450 mm a^{-1}, the net accumulation at 5500 m is 260 mm a^{-1}.

Field measurements of climate parameters, sublimation rates, and results from a 39 m long ice core taken on the summit plateau in February 1999 provide independent data to assess the quality of the model results. In the ice core at 5500 m, the ^{3}H tritium peak of 1964 is found at the depth of 10.00 m water equivalent in (Schotterer, 2000, personal communication), suggesting mean annual net accumulation rates of 290 mm water equivalent at the drilling site during the last 35 years

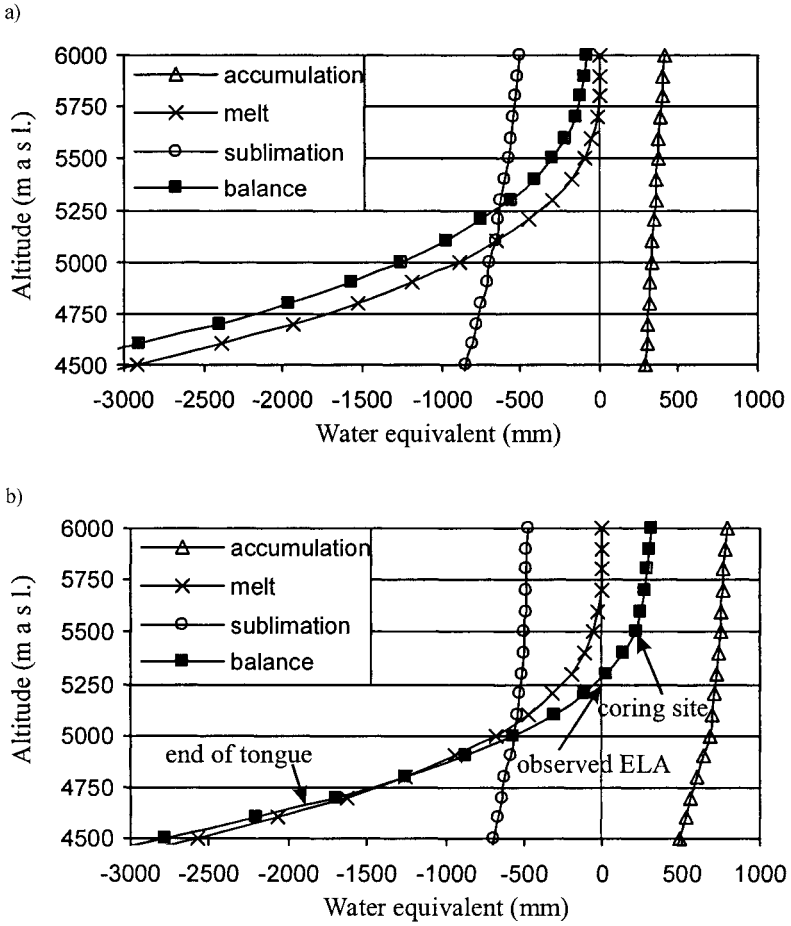

Figure 5. (a) Model results for the mean annual mass balance terms in different altitudes of the Cerro Tapado glacier as computed using the actual climatic data of the region (station data, Table I). The mass balance is negative up to 6000 m altitude and shows the regional lack of glaciers even in the continuous permafrost belt. (b) Shows the results computed with increased accumulation (total of 750 mm a^{-1} at 5500 m, 170 mm due to re-deposition or local effects). The calculated mass balance turns to positive values above 5280 m altitude which compares favorably with field observations and mass balance calculations obtained from chemical and radio-isotope data of the ice core (Table III, Ginot et al., 2002).

(Table III). This compares well with the modeled value of 260 mm a^{-1}. Although melt was calculated to be 60 mm a^{-1} and was observed (ice lenses in the firn, little frozen lakes) on the summit plateau, we suggest that these values remain neutral with regard to the mass balance. Firn and ice temperatures are between – 8.5 °C and –12 °C (Ginot et al., 2002) and small ice lenses in the upper part of the core suggest immediate re-freezing of the melt water and thus marginal mass loss.

Lysimeter measurements (February 11–16, 1999) yielded mean daily sublimation rates of 1.89 mm at 5550 m (Figure 4 and Table III), which compares favorably with the modeled values. Based on enrichment factors of chemical species and stable isotopes in the snow, Ginot et al. (2002) calculated sublimation rates of 1.85 mm d^{-1} for the same period of time; furthermore, cumulative sublimation between the last big snow fall (September 1998) and our field trip (February 1999) was calculated to be 310 mm, which is also close to the modeled value of 320 mm.

The presence of the Tapado glacier in a generally glacier-free environment emphasizes the local atypical climatic-glaciological conditions with increased accumulation rates. We consider two processes to be relevant. First, re-deposition of snow and snow-cornices along the crest was observed and may account for the locally enhanced accumulation rates. Second, Co. Tapado is located directly in front of the Paso del Agua Negra. Ammann (1996) showed that moisture is preferentially transported along valleys, which results in locally enhanced cloud cover and precipitation.

In summary, the good match between model results and independent glaciological field observations allows us to conclude that the parametrization of the climate input data, the local lapse rates, and the empirical-statistical mass balance model are robust and suitable enough to reconstruct glaciological features and thus mass balance terms under modern conditions in this area. This provides the basis for applying the model to late Pleistocene conditions.

4.2. THE PLEISTOCENE GLACIATION IN THE ENCIERRO VALLEY

The results for the best-fit paleoclimate scenarios drawn from two case study glaciers in the Encierro valley (Encierro and Las Palas) are listed in Table IV and Figure 6. There is a good agreement between both examples. The late Pleistocene glacier stage referred herein is the *Phase II* glaciation described in Jenny and Kammer (1996). The reconstructed mass balance – elevation distributions suggest late Pleistocene ELAs at 4305 ± 35 m (Encierro) and at 4325 ± 20 m (Las Palas), which implies a late Pleistocene ELA depression of 1000 m if compared with the modern ELA at Co. Tapado. Similar values were found elsewhere in the Andes (Hastenrath, 1971; Seltzer, 1992, 1993; Jenny and Kammer, 1996).

The model results show that sublimation is the dominant ablation term above 4500 m altitude. The reconstructed AAR (Accumulation Area Ratio) were calculated to be 0.62 (Encierro) and 0.60 (Las Palas) respectively. The modeled mass balance gradients in the ablation area (6.5 kg m^{-2} m^{-1} at Encierro, 7.1 kg m^{-2} m^{-1} at Las Palas) are relatively low and hint at relatively cold environments.

The results for the best-fit paleoclimate scenario suggest a precipitation increase of about 550 ± 150 mm a^{-1} (compared to today), accompanied by a major temperature depression of 5.7 ± 0.75 °C (Encierro) and 5.6 ± 0.8 °C (Las Palas) at 4000 m. This paleoclimate scenario generates glaciers that match the geometry and glaciological features observed in the field. If the distinction is made between local

Table IV

Best-fit late Pleistocene climate scenario and glaciological conditions for both case-study glaciers calculated for 4000 m a s l. The given range is calculated based on an accuracy of ±10% for geometrical model parameters of the glacier and ±20% for the ice flow parameters

		Encierro	Δ change values	Las Palas	Δ change values
Temperature °C	annual mean	–4.6 (+–0.75)	–5.7 (+–0.75)	–4.4 (+–0.8)	–5.6 (+–0.8)
Precipitation mm	annual mean	990 (+–150)	+550 (+–150)	980 (+–140)	+560 (+–140)
	winter (%)	50 (+–50)		50 (+–50)	
ELA	m a s l.	4305 (+–35)	∼−1000	4325 (+–20)	∼−1000
	p_{ELA} (mm)	1026 (+–150)		1020 (+–140)	
	t_{ELA} (°C)	–6.7 (+–0.55)		–6.6 (+–0.55)	
AAR		0.62 (+–0.02)		0.60 (+–0.02)	
Mass bal. grad. kg m^{-2} m^{-1}	(abl. area)	6.5 (+–0.55)		7.1 (+–0.65)	

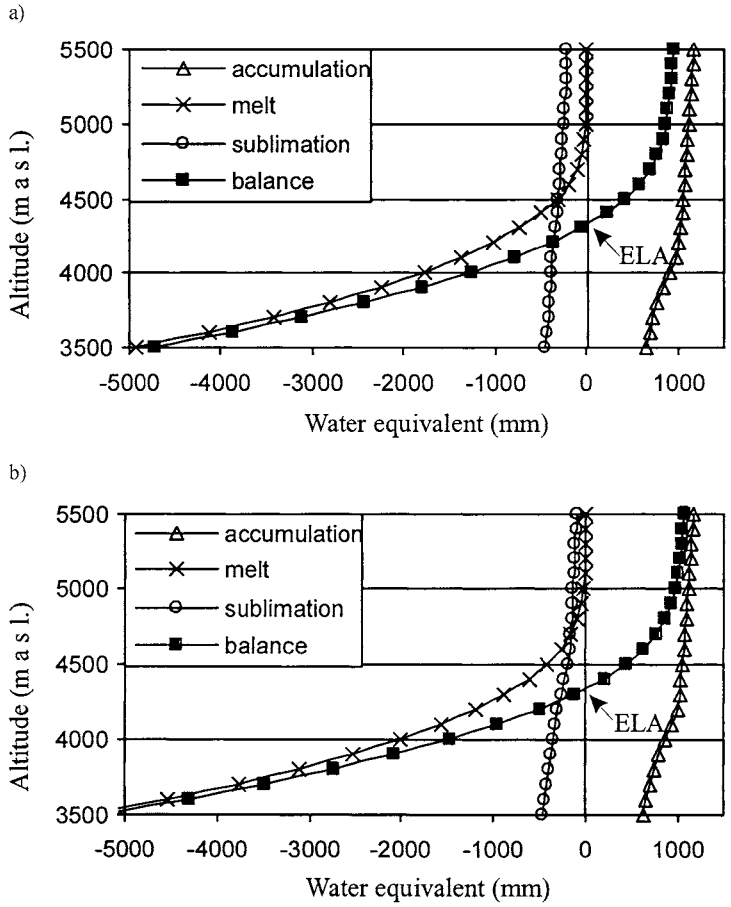

Figure 6. Best-fit mean annual mass balance – elevation distributions for the late Pleistocene maximum glacier advances at Encierro (a) and Las Palas (b). The calculated ELAs are located at 4305 m (Encierro) and 4325 m (Las Palas). Mean annual balance gradients in the ablation area are between 6.5 kg m^{-2} m^{-1} and 7.1 kg m^{-2} m^{-1}, the model AAR is ~0.60, which suggests that the former glaciers existed under a relatively cold and moderately humid climate.

and regional effects of the temperature depression (using Equation (1)), one can conclude that local temperature effects (due to local cloudiness, precipitation and latent heat) account only for about –0.6 °C, thus indicating that a large proportion (ca. –5 °C) of the total temperature reduction is due to (supra)regional effects.

The model was also run for changing seasonality and different proportions of winter and summer precipitation. Interestingly, given the confidence range for our sensitivity tests (±10% for geometrical parameters, ±20% for ice flow parameters), the results (50 ± 50% winter precipitation) are indicative for neither winter nor summer precipitation (Table IV). This is very different from the late Pleistocene glaciers north of the Arid Diagonal, where winter precipitation at 18° S was calcu-

lated to remain below 30% of the total annual precipitation (Kull and Grosjean, 2000).

5. Paleoclimatic Implications

5.1. CHRONOLOGY AND CLIMATES DURING THE MAXIMUM GLACIER ADVANCES NORTH AND SOUTH OF THE ARID DIAGONAL

A comparison between the results of the glaciers south of the Arid Diagonal (at 29° S, discussed above) with those north of the Arid Diagonal (18–22° S, Kull, 1999; Kull and Grosjean, 2000) gives rise to a number of arguments allowing us to postulate very different paleoclimatic conditions for each area and thus to propose a different timing of the observed glacier advances (Figure 7). This is an important issue because direct dating of the glacial advances in the southern part (29° S) has not been successful so far, whereas the maximum glacier advances in the north (18–22° S) are dated to late-glacial times (Clayton and Clapperton, 1997).

The glaciers in the southern area (29° S) developed during cold and moderately humid conditions, while moderately cold but very humid conditions triggered maximum advances in the tropical part (18–22° S). In particular, regional temperature depressions, considered a suitable large-scale climate indicator, were different in each test areas. In the north, $\Delta T_{\text{regional}}$ depressions of –1.8 to –3.0 °C seem reasonable for a late-glacial scenario, whereas the $\Delta T_{\text{regional}}$ of –5.1 °C observed in the southern test area are more consistent with a LGM ($25 - 18^{14}$C ka?, marine isotope stage MIS 2) scenario.

Interestingly, differences between the north and the south are also found in the glaciological parameters. Mass balance gradients in the ablation area of the glaciers around 29° S are much lower (6.5–7.1 kg m^{-2} m^{-1}) than those of the case study glaciers in the north (8.8–9.2 kg m^{-2} m^{-1}). The values for the northern glaciers are typical for (sub)tropical glaciers with a dry cold winter and a wet warm summer (Kaser, 1996; Kaser et al., 1996; Kaser and Georges, 1999; Kull, 1999; Kull and Grosjean, 2000), whereas the values for the southern glaciers are typical for generally colder and drier climates.

The results for the southern case study glaciers (29° S) are consistent with findings from South-Central Chile (33° S–43° S), where the maximum glacier expansion is documented for full glacial times and reconstructed temperature depressions are in a comparable range (Denton et al., 1999; Espizua, 1999; Farrera et al., 1999; Heusser et al., 1999; Moreno et al., 1999). Also the doubling of annual precipitation is consistent with findings by Caviedes (1990), Lamy et al. (1998) and Heusser et al. (1999) for South and Central Chile during full glacial times.

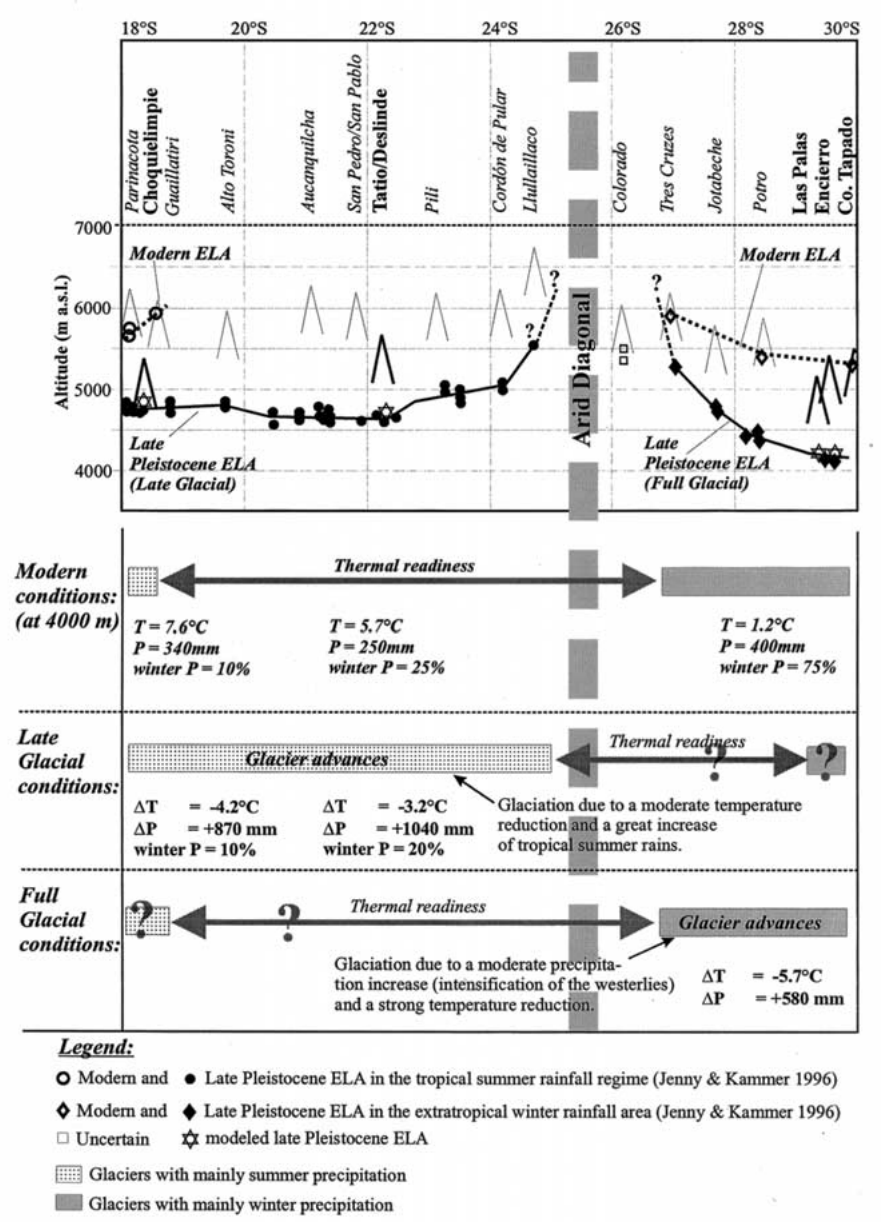

Figure 7. Synthesis of the modern, late-glacial, LGM climate and glaciological information along the transect between 18 and 30° S as drawn from the climate-glacier model (Kull, 1999; Kull and Grosjean, 2000). ΔT and ΔP are compared to modern conditions. The transect shows large meridional fluctuations of the tropical summer precipitation regime with the corresponding glaciers during late-glacial very humid and moderately cold conditions. The northern boundary of the extratropical winter precipitation belt seems to have been locked at 27° S during late Quaternary times, whereas the much steeper meridional precipitation gradients generated widespread glaciation south of 27° S during LGM (?) times under moderately humid but very cold conditions. The core area of the Atacama Desert between 25 and 27° S seems not to be affected by late Pleistocene/Holocene moisture changes. Evidence of glaciation is still negative in this part of the transect.

5.2. ATMOSPHERIC CIRCULATION DURING LATE PLEISTOCENE TIMES

Today, precipitation in the research area at 29° S arrives as frontal winter precipitation from Pacific moisture sources. In contrast to the view of Markgraf (1989, 1993) and Markgraf et al. (1992), our findings support the existence of an intensified Westerly circulation in this area during LGM times (Heusser, 1990; Kerr and Sugden, 1994; Heusser et al., 1999; Moreno et al., 1999). Tropical moisture in the western Andes at 29° S was likely reduced during this time, since the paleoenvironments adjacent to the North and East (source area of the moisture) suggest dry conditions and thus interrupted easterly moisture transport for that period (Kull and Grosjean, 1998; Ledru et al., 1998; Sifeddine et al., 1998; Thompson et al., 1998; Behling et al., 2000; Betancourt et al., 2000; Grosjean et al., 2001). Enhanced westerly circulation was inferred from marine sediment cores along the coast of Central Chile (Lamy et al., 1998). However, the fact that the northern boundary of the modern and the Pleistocene glaciation is found at the same latitude (Figure 7) strongly suggests that the northern boundary of the westerlies did not shift towards lower latitudes, but remained very stable in its current position, although intensified and with much steeper meridional gradients. Interestingly, this feature of atmospheric circulation is very different from northern hemisphere observations during LGM times. Evidence for a locked position of the northern boundary of the westerlies was also found in recent GCM (Global Circulation Model) model runs where westerly storm tracks, the centers of cyclogenesis and cyclolysis on the southern hemisphere were investigated for LGM times (Wyrwoll et al., 2000).

Our results, however, do not allow full exclusion of additional precipitation from continental moisture sources. These might be related in the present and in the past to mobile polar highs (PMHs), i.e., outbreaks of polar air masses along the east side of the Andes (Servant et al., 1993; Martin et al., 1997). In their study of the climatology of southern hemisphere extratropical cyclones, Jones and Simmonds (1993) concluded that the chief mechanisms contributing to the maximum of cyclone density and genesis in the lee of the Andes (Chaco region) are topographical and thermal effects, i.e., the damming effect of the Andean mountain chain, and low-level advections of warm air from the northwest playing the major role. This observation is interesting because the stable topography of the Andes during the late Quaternary would offer an explanation for the locked position of the westerlies. This seems to be a characteristic feature of the N–S Andean mountain chain, that is perpendicular to the zonal mid-latitude air flow of the southern hemisphere and thus different from the northern mid-latitudes (e.g., Europe and northern Africa), where large displacements of the westerlies are a common circulation feature during late Quaternary times.

The stable position of the northern boundary of winter precipitation further implies that the core area of the Arid Diagonal adjacent to the north also remained in the same position during the late Quaternary. Indeed, evidence of Pleistocene glaciation between 25–27° S is still missing or highly ambiguous (Figure 7, Jenny

and Kammer, 1996), and first exposure age dates using cosmogenic ^{3}He and ^{21}Ne of erratic blocks at 27° S suggest much older ages for the last major glaciation of about 200 kyr (Hammerschmidt, 1999, personal communication). Furthermore, the fingerprint of the late-glacial/early Holocene paleolake transgression (Tauca and Coipasa Phases, Sylvestre et al., 1999), that is very pronounced on the southern Altiplano of S Bolivia, NW Argentina and northern Chile, disappears in the western Andes south of 25° S (Grosjean et al., 1995, Geyh et al., 1999). All of these observations suggest that the area between 25–27° S was not influenced by the major humidity changes during late Quaternary times from the tropical precipitation belt nor by changes in the extratropical westerlies precipitation belt.

6. Conclusions

A glacier-climate model was used to reconstruct climate conditions that sustained late Pleistocene glaciers in the south-central Andes of northern Chile at 29° S, i.e., south of the Arid Diagonal. The model was first successfully tested against the recent glacier on Cerro Tapado at 30° S.

The glacier on Cerro Tapado at 5500 m is an isolated atypical ice mass, surrounded by ice-free mountains as high as 6000 m. The model results for the mass balance terms (accumulation, sublimation and melt) compare favorably with field measurements and independent mass balance calculations based on enrichment factors of chemical species and isotope data from an ice core taken on the summit plateau. Thus we conclude that the parametrization of the climate input data, the lapse rates, and the empirical-statistical mass balance model are robust. These are used to describe glaciological features as well as mass balance terms under modern conditions in this area and thereby provide a basis for applying the model to late Pleistocene conditions.

The best-fit climate scenarios (annual values) for two test sites (Encierro, Las Palas) suggest a moderate precipitation increase by a factor of 2 ($\Delta P = +580$ mm) and large temperature depressions ($\Delta T = -5.7$ °C), whereby regional temperature depressions account for the largest proportion and local temperature effects due to local cloudiness and latent heat are minor ($\Delta T_{\text{regional}} = -5.1$ °C, $\Delta T_{\text{local}} = -0.6$ °C). Both, this paleoclimate scenario and mass balance gradients for the ablation area are significantly different from the very moist, but moderately cold, climate conditions calculated for the Pleistocene glaciers north of the arid Diagonal (between 18 and 22° S). Therefore, we hypothesize that maximum glacier advances in the areas north and south of the Arid Diagonal were triggered by different large-scale climates and thus are not contemporaneous. The glaciers north of the Arid Diagonal (18–22° S) correspond to a late-glacial climate, confirmed by ^{14}C dates. These glaciers were synchronous with paleolake transgressions, whereas the glaciers south of the Arid Diagonal (29° S) correspond more closely to a LGM climate and MIS2. Direct dating of this maximum advance is still lacking. Similar differences

in the timing of the maximum glacier extent (late glacial – LGM) are also evident on the northern hemisphere (Mexico; Heine, 1994; Hastenrath, 1995).

The driest part of the Arid Diagonal remained very stable between 25 and 27° S. In this part of our transect, evidence for Pleistocene glaciation has yet to be found, and evidence of late-glacial paleolake transgressions is restricted to the area adjacent to the north. We suggest that either this area was not subject to late Quaternary moisture changes, or that the changes remained below the critical threshold values necessary for detection by current glaciological tools.

Our model results for the two case study glaciers at 29° S are not conclusive with regard to seasonality of precipitation (winter and summer). However, comparison with regional paleodata supports enhanced winter precipitation with Pacific moisture sources. Interestingly, the northern boundary of the winter precipitation belt remained very stable at 27° S during late Pleistocene and Holocene times. The N–S gradients of Pleistocene ELAs – and thus precipitation – were, however, much steeper than today. This feature also appears in GCM runs investigating LGM storm tracks. Analysis of modern cyclone activity and centers of cyclogenesis in the southern hemisphere suggest that topographical and thermal effects of the N–S Andean mountain chain play a key-role with regard to the position of maximum cyclone density. Given constant topography during the last 20 kyr, this observation may offer an explanation for the locked position of the westerlies in this region during late Quaternary times. This is fundamentally different from the situation in the mid-latitudes of the northern hemisphere.

Acknowledgements

This study is part of the Swiss NSF project ‘Paleoclimate of the central Andes’ (NF 20-056908.99) awarded to Heinz Veit. The methodological and logistical support provided by Georg Kaser, Hans Oerlemans, Bernard Pouyaud, Pierre Ribstein, Bruno Messerli, Heinz Gäggeler, Margit Schwikowski, Ulrich Schotterer, Patrick Ginot and Marcela Espinoza (DIFROL, Chile) is thankfully acknowledged.

References

Ammann, C.: 1996, ‘Climate Change in den trockenen Anden: Aktuelle Niederschlagsmuster’, *Geographica Bernensia* G**46**, 81–127.

Behling, H., Arz, H. W., Pätzold, J., and Wefer, G.: 2000, ‘Late Quaternary Vegetational and Climate Dynamics in Northeastern Brazil, Inferences from Marine Core GeoB 3104-1’, *Quat. Sci. Rev.* **19**, 981–994.

Betancourt, J. L. C., Latorre, J. A., Rech, J., Quade and Rylander, K. A.: 2000, ‘A 22,000-Yr Record of Monsoonal Precipitation from Northern Chile‘s Atacama Desert’, *Science* **289**, 1542–1546.

Bradbury, J. P., Grosjean, M., Stine, S., and Sylvestre, F.: 2001, ‘Full and Late Glacial Lake Records along the PEP 1 Transect: Their Role in Developing Interhemispheric Paleoclimate Interactions’, in Markgraf, V. (ed.), *Interhemispheric Climate Linkages*, Academic Press, pp. 265–291.

Budd, W. F.: 1969, 'The Dynamics of Ice Masses', in *Australian National Antarctic Research Expeditions*, Scientific Report **108**, Melbourne.

Caviedes, C. N.: 1990, 'Rainfall Variation, Snowline Depression and Vegetational Shifts in Chile during the Pleistocene', *Clim. Change* **16**, 9–114.

Clayton, J. D. and Clapperton, C. M.: 1997, 'Broad Synchrony of a Late-Glacial Glacier Advance and the Highstand of Palaeolake Tauca in the Bolivian Altiplano', *J. Quat. Sci.* **12**, 169–182.

Denton, G. H., Heusser, C. J., Lowell, T. V., Moreno, P. I., Andersen, B. G., Heusser, L. E., Schlüchter, C., and Marchant, D. R.: 1999, 'Interhemispheric Linkage of Paleoclimate during the Last Glaciation', *Geogr. Ann.* **81**, 107–153.

Espizua, L. E.: 1999, 'Chronology of Late Pleistocene Glacier Advances in the Rio Mendoza Valley, Argentina', *Glob. Plan. Change* **22**, 193–200.

Farrera, I., Harrison, S. P., Prentice, I. C., Ramstein, G., Guiot, J., Bartlein, P. J., Bonnefille, R., Bush, M., Cramer, W., von Grafenstein, U., Holmgren, K., Hooghiemstra, H., Hope, G., Jolly, D., Lauritzen, S.-E., Ono, Y., Pinot, S., Stute, M., and Yu, G.: 1999, 'Tropical Climates at the Last Glacial Maximum: A New Synthesis of Terrestrial Palaeoclimate Data. I. Vegetation, Lake-Levels and Geochemistry', *Clim. Dyn.* **15**, 823–856.

Geyh, M. A., Grosjean, M., Nunez, L., and Schotterer, U.: 1999, 'Radiocarbon Effect and the Timing of the Late-Glacial/Early Holocene Humid Phase in the Atacama Desert (Northern Chile)', *Quat. Res.* **52**, 143–153.

Ginot, P., Kull, C., Schwikowski, M., Schotterer, U., and Gäggeler, H. W.: 2002, 'Effects of Post-Depositional Processes on Snow Composition of a Subtropical Glacier (Cerro Tapado, Chilean Andes)', *J. Geophys. Res.*, in press.

Grosjean, M., Geyh, M., Messerli, B., and Schotterer, U.: 1995, 'Late-Glacial and Early Holocene Lake Sediments, Groundwater Formation and Climate in the Atacama Altiplano', *J. Paleolimnol.* **14**, 341–252.

Grosjean, M., van Leeuwen, J. F. N., van der Knaap, W. O., Geyh, M. A., Ammann, B., Tanner, W., Messerli, B., and Veit, H.: 2001, 'A 22,000 ^{14}C Yr BP Sediment and Pollen Record of Climate Change from Laguna Miscanti 23° S, Northern Chile', *Glob. Plan. Change* **28**, 35–51.

Hastenrath, S.: 1971, 'On the Pleistocene Snow-Line Depression in the Arid Regions of the South American Andes', *J. Glaciol.* **3**, 255–267.

Hastenrath, S.: 1995, *Climate Dynamics of the Tropics*, Kluwer Academic Publ., cop. Dordrecht, p. 488.

Hastenrath, S. and Kutzbach, J. E.: 1985, 'Late Pleistocene Climate and Water Budget of the South American Altiplano', *Quat. Res.* **24**, 249–256.

Heine, K.: 1994, 'The Late Glacial Moraine Sequences in Mexico: Is There Evidence for the Younger Dryas Event?', *Palaeogeogr. Palaeoclimatol. Palaeoecol.* **112**, 113–123.

Heusser, C. J.: 1990, 'Ice Age Vegetation and Climate of Subtropical Chile', *Palaeogeogr. Palaeoclimatol. Palaeoecol.* **80**, 107–127.

Heusser, C. J., Heusser, L., and Lowell, T. V.: 1999, 'Paleoecology of the Southern Chilean Lake District-Isla Grande de Chiloé during Middle-Late Llanquihue Glaciation and Deglaciation', *Geogr. Ann.* **81**, 231–284.

Jenny, B. and Kammer, K.: 1996, 'Climate Change in den trockenen Anden: Jungquartäre Vergletscherung', *Geographica Bernensia* G**46**, 1–80.

Jones, D. A. and Simmonds, I.: 1993, 'A Climatology of Southern Hemisphere Extratropical Cyclones', *Clim. Dyn.* **9**, 131–145.

Kaser, G.: 1996, 'Gletscher in den Tropen – ein Beitrag zur Geographie der tropischen Hochgebirge', Habilitationsschrift, Universität Innsbruck. p. 254.

Kaser, G., Hasthenrath, S., and Ames, A.: 1996, 'Mass Balance Profiles on Tropical Glaciers', *Z. Gletscherk. Glazialgeol.* **32**, 75–81.

Kaser, G. and Georges, Ch.: 1999, 'On the Mass Balance of Low Latitude Glaciers with Particular Consideration of the Peruvian Cordillera Blanca', *Geogr. Ann.* **81**, 643–651.

Kerr, A. and Sugden, D.: 1994, 'The Sensitivity of the South Chilean Snowline to Climatic Change', *Clim. Change* **28**, 255–272.

Kull, C.: 1999, 'Modellierung paläoklimatischer Verhältnisse basierend auf der jungpleistozänen Vergletscherung in Nordchile – Ein Fallbeispiel aus den Nordchilenische Anden', *Z. Gletscherk. Glazialgeol.* **35**, 35–64.

Kull, C. and Grosjean, M.: 1998, 'Albedo Changes, Milankovitch Forcing and Late Quaternary Climate Changes in the Central Andes', *Clim. Dyn.* **14**, 871–881.

Kull, C. and Grosjean, M.: 2000, 'Late Pleistocene Climate Conditions in the North Chilean Andes Drawn from a Climate-Glacier Model', *J. Glaciol.* **46**, 622–632.

Lamy, F., Hebbeln, D., and Wefer, G.: 1998, 'Late Quaternary Precessional Cycles of Terrigenous Sediment Input off the Norte Chico, Chile (27.5° S) and Paleoclimatic Implications', *Palaeogeogr. Palaeoclimatol. Palaeoecol.* **141**, 233–251.

Ledru, M.-P., Bertaux, J., Sifeddine, A., and Suguio, K.: 1998, 'Absence of Last Glacial Maximum Records in Lowland Tropical Forests', *Quat. Res.* **49**, 233–237.

Markgraf, V.: 1989, 'Reply to Heusser's "Southern Westerlies during the Last Glacial Maximum" ', *Quat. Res.* **31**, 426–432.

Markgraf, V.: 1993, 'Climatic History of Central and South America since 18,000 Yr B.P.: Comparison of Pollen Records and Model Simulations', in Wright H. E. et al. (eds.), *Global Climates since the Last Glacial Maximum*, University of Minnesota Press, pp. 357–385.

Markgraf, V., Dodson, J. A., Kershaw, P. A., McGlone, M. S., and Nicholls, N.: 1992, 'Evolution of the Late Pleistocene and Holocene Climates in the Circum-South Pacific Land Areas', *Clim. Dyn.* **6**, 193–211.

Martin, L., Bertaux, J., Corrège, T., Ledru, M. P., Mourguiart, P., Sifeddine, A., Soubiès, F., Wirrmann, D., Suguio, K., and Turq, B.: 1997, 'Astronomical Forcing of Contrasting Rainfall Changes in Tropical South America between 12,400 and 8,800 Cal Yr B.P.', *Quat. Res.* **47**, 117–122.

Messerli, B., Ammann, C., Geyh, M., Grosjean, M., Jenny, B., Kammer, K., and Vuille, M.: 1996, 'Current Precipitation, Late Pleistocene Snow Line and Lake Level Changes in the Atacama Altiplano (18° S–28°/29° S)', *Bamberger Geographische Schriften* **15**, 17–35.

Minetti, J. L., Barbieri, P. M., Carletto, M. C., Poblete, A. G., and Sierra, E. M.: 1986, 'El régimen de precipitatiòn de la provincia de San Juan. – Informe técnico 8', CIRSAJ-CONICET, San Juan.

Moreno, P. I., Lowell, T. V., Jacobson Jr., G. L., and Denton, G. H.: 1999, 'Abrupt Vegetation and Climate Changes during the Last Glacial Maximum and Last Termination in the Chilean Lake District: A Case Study from Canal de la Puntilla (41° S)', *Geogr. Ann.* **81**, 285–311.

Oerlemans, J.: 1997, 'A Flowline Model for Nigardsbreen, Norway: Projection of Future Glacier Length Based on Dynamic Calibration with the Historic Record', *Ann. Glaciol.* **24**, 382–389.

Paterson, W. S. B.: 1994, *The Physics of Glaciers* 3rd edn., Pergamon, Oxford, p. 480.

Seltzer, G. O.: 1992, 'Late Quaternary Glaciation of the Cordillera Real, Bolivia', *J. Quat. Sci.* **7**, 87–98.

Seltzer, G. O.: 1993, 'Late Quaternary Glaciation as a Proxy for Climate Change in the Central Andes', *Mount. Res. Dev.* **13**, 129–138.

Servant, M., Maley, J., Turcq, B., Absy, M-L., Brenac, P., Fournier, M., and Ledru, M-P.: 1993, 'Tropical Forest Changes during the Late Quaternary in African and South American Lowlands', *Glob. Plan. Change* **7**, 25–40.

Sicart, J. E., Wagnon, P., Gallaire, R., Francou, B., Ribstein, P., Pouyaud, B., and Baldivieso, H.: 1998, 'Mesures météorologiques, hydrologiques et glaziologiques sur le glacier du Zongo, Année Hydrologique 1996–97', *Informe No* **57**, ORSTOM La Paz. p. 119.

Sifeddine, A., Bertaux, J., Mourguiart, P., Martin, L., Disnar, J.-R., Laggoun-Défarge, F., and Argollo, J.: 1998, 'Etude de la sédimentation lacustre d'un site de forêt d'altitude des Andes centrales (Bolivie). Implications paléoclimatiques', *Bull. Soc. Géol. France* **169**, 395–402.

Sylvestre, F., Servant, M., Servant-Vildary, S., Causse, C., Fournier, M., and Ybert, J-P.: 1999, 'Lake-Level Chronology on the Southern Bolivian Altiplano (18–23° S) during Late-Glacial Time and the Early Holocene', *Quat. Res.* **51**, 54–66.

Thompson, L. G., Davis, M. E., Mosley-Thompson, E., Sowers, T. A., Henderson, K. A., Zagorodnov, V. S., Lin, P.-N., Mikhalenko, V. N., Campen, R. K., Bolzan, J. F., Cole-Dai, J., and Francou, B.: 1998, 'A 25,000-Year Tropical Climate History from Bolivian Ice Cores', *Science* **282**, 1858–1864.

Thompson, L. G., Mosley-Thompson, E., Davis, M. E., Lin, P. N., Henderson, K. A., Coledai, J., Bolzan, J. F., and Liu, K.: 1995, 'Late Glacial Stage and Holocene Tropical Ice Core Records from Huascarán, Peru', *Science* **269**, 46–50.

Veit, H.: 1995, 'Jungquartäre Landschafts- und Klimaentwicklung der zentralen Anden und ihres westlichen Vorlandes: Kenntnisstand und Probleme', *Geomethodica* **20**, 163–194.

Veit, H.: 1996, 'Southern Westerlies during the Holocene Deduced from Geomorphological and Pedological Studies in the Norte Chico, Northern Chile (27–33° S), *Palaeogeogr. Palaeoclimatol. Palaeoecol.* **123**, 107–119.

Vuille, M.: 1996, 'Zur raumzeitlichen Dynamik von Schneefall und Ausaperung im Bereich des südlichen Altiplano, Südamerika', *Geographica Bernensia* G**45**, 118.

Vuille, M. and Ammann, C.: 1997, 'Regional Snowfall Patterns in the High, Arid Andes (South America)', *Clim. Change* **36**, 413–123.

Wagnon, P., Ribstein, P., Francou, B., and Pouyaud, B.: 1999, 'The Annual Cycle of the Energy Balance of a Bolivian Glacier – Implications on Tropical Glaciology', *J. Geophys. Res.* **104**, 3907–3924.

Wyrwoll, K.-H., Dong, B., and Valdes, P.: 2000, 'On the Position of Southern Hemisphere Westerlies at the Last Glacial Maximum: An Outline of AGCM Simulation Results and Evaluation of their Implications', *Quat. Sci. Rev.* **19**, 881–898.

(Received 18 July 2000; in revised form 9 July 2001)